Synthesis and structural characterization of ruthenium(II) complexes of histidine and methionine derivatives

W. S. Sheldrick* and R. Exner

Lehrstuhl für Analytische Chemie, Ruhr-Universität Bochum, Postfach 10 21 48, D-4630 Bochum 1 (FRG)

(Received October 4, 1991)

Abstract

The L-histidinate complexes [RuCl(L-his)(diene)] (diene = nbd (**1**), cod (**2**)) may be prepared by reaction of $[RuCl_2(dien)]_n$ with L-hisH in aqueous solution at reflux. An X-ray analysis of **1** established that the histidinate anion is present as a facial tridentate ligand with the amino nitrogen sited *trans* to chlorine. Reaction of $[RuCl_2(PPh_3)_3]$ with D,L-histidine in methanol at reflux leads to the formation of $[RuCl(D,L\text{-his})(PPh_3)_2]$ (**3**), which also contains a facially coordinated tridentate histidinate ligand (X-ray analysis). In contrast to **1**, the coordinating imidazole nitrogen is now in *trans* position to the chlorine atom. The complexes $[RuCl_2(L\text{-hisme})(PPh_3)_2]$ (**4**), $[RuCl(D,L\text{-met})(PPh_3)_2]\cdot CH_3OH$ (**5**) and $[RuCl(L\text{-metme})_2(PPh_3)]Cl\cdot PPh_3$ (**6**) were characterized by spectroscopic studies and in the case of **6** by an X-ray structural analysis. In the latter bis-chelate complex the thioether sulfur atoms adopt coordination sites *trans* to an amino nitrogen and the PPh_3 phosphorus, respectively. In aqueous or methanolic solution **6** is readily oxidized by traces of oxygen. The analogous ruthenium(III) reaction product for L-methionine ethyl ester (L-metet), $[RuCl_3(L\text{-metet})(PPh_3)]$ (**7**) was characterized by X-ray analysis. The electrochemistry of **4** and **7** has been studied.

Introduction

The reaction of $[RuCl_2(diene)]_n$ (diene = norbornadiene (nbd), 1,5-cyclooctadiene (cod)) with α-amino acids (aaH) such as glycine (glyH), D,L-alanine (D,L-ala) or L-phenylalanine (L-phe) in aqueous solution at reflux leads to the formation of complexes of the type $[Ru(aa)_2(diene)]$ [1, 2]. Analogous complexes $[Ru(aa)_2(PPh_3)_2]$ (aaH = glyH, L-alaH, LvalH) may be prepared by the reaction of $[RuCl_2(PPh_3)_3]$ with aaH in methanol at reflux [3]. Crystal structure determinations for Δ-$[Ru(L\text{-phe})_2(nbd)]$ [2] and Δ-$[Ru(L\text{-ala})_2(PPh_3)_2]$ [3] confirmed the presence of two five-membered chelate rings with N(amine),O(carboxyl)-coordination of the amino acidate ligands. We have recently extended these studies to the reaction of $[RuCl_2(diene)]_2$ with the sulfur containing amino acids or esters, D,L-methionine methyl ester (D,L-metme), D,L-methionine (D,L-metH), D,L-penicillamine (D,L-penH) and D,L-cysteine (D,L-cysH) [4]. X-ray analyses for $[RuCl_2(D,L\text{-metme})(nbd)]$, [RuCl(D,L-met)(nbd)] and $[Ru(D,L\text{-penH}_{-1})(nbd)]_2$ have established the amino acidate ligands as bi-, tri- and tetradentate, respectively, with S,N-, S,N,O- and S,S,N,O-coordination. In contrast IR and ^1H NMR spectroscopic data indicate that the carbonyl groups in dimeric $[RuCl(D,L\text{-cys})(cod)]_2$ are protonated and do not participate in coordination of the Ru atoms.

We now report the preparation and structural characterization of the diene–ruthenium(II) complexes of L-histidine (L-hisH) [RuCl(L-his)(nbd)] (**1**) and [RuCl(L-his)(cod)] (**2**). The histidine imidazole ring has been found to coordinate ruthenium(II) in $[RuCl(L\text{-hisH})(\eta^6\text{-}C_6H_6)]Cl$ [5]. We have also extended our studies on the reaction of $[RuCl_2(PPh_3)_3]$ with α-amino acids to cover histidine and methionine derivatives. In this work we present X-ray structural studies on $[RuCl(D,L\text{-his})(PPh_3)_2]\cdot 1\frac{1}{2}CH_3OH$ (**3**) $[RuCl(L\text{-metme})_2(PPh_3)]Cl\cdot PPh_3$ (**6**) and the ruthenium(III) complex $[RuCl_3(L\text{-metet})(PPh_3)]$ (**7**). The structural characterization of triphenylphosphine–ruthenium(II) complexes of the peptides diglycine and triglycine has been recently reported [6].

Experimental

All reactions with the exception of the preparation of **7** were carried out under an inert gas atmosphere. Solvents were dried and distilled before use. IR spectra were recorded as 1% KBr discs on a Perkin-Elmer 297 spectrometer. ^1H NMR spectra were recorded on a

*Author to whom correspondence should be addressed.

0020-1693/92/$5.00

Bruker AM 400 spectrometer at 20 °C. Cyclic voltammograms for **3** and **7** were measured at scan rates from 0.01 to 1 V s^{-1} for an approximate concentration of the electro-active component of 10^{-3} M. The complexes were investigated in CH_2Cl_2 solution containing 0.1 M tetra-n-butylammonium hexafluorophosphate as supporting electrolyte at a glassy-carbon electrode and an Ag/AgCl reference electrode. The redox potentials were referenced versus the ferrocenium/ferrocene couple as internal standard [7]. Elemental analyses were performed with a Perkin-Elmer 240. The α-amino acids and esters were purchased from Sigma Chemie GmbH and used as received. $RuCl_3 \cdot 3H_2O$ was a gift from Degussa AG. $[RuCl_2(cod)]_n$, $[RuCl_2(nbd)]_n$ [8–10] and $[RuCl_2(PPh_3)_3]$ [11] were prepared as described previously.

Preparation of complexes 1–7

[RuCl(L-his)(nbd)]·CH_3OH (1)

A mixture of 238 mg (0.90 mmol) $[RuCl_2(nbd)]_n$ and 145 mg (0.93 mmol) L-histidine in 15 ml H_2O was heated with stirring for 15 h at reflux. The orange–yellow solution was filtered and dried in vacuum. The solid was dissolved in 4 ml methanol. Yellow crystals of **1** were obtained by cooling the solution to −30 °C. Yield 217 mg (60%). *Anal.* Found: C, 40.4; H, 4.81; N, 10.1. Calc. for $C_{14}H_{20}N_3O_3ClRu$ (*M*, 414.9): C, 40.5; H 4.86; N 10.1%. IR: 3230 m, 3145s $\nu(NH_2)$, 1620s $\nu(CO)$, 1600s $\delta(NH_2)$ cm^{-1}. ^1H NMR (D_2O/DSS): 1.69 (m, 2H, nbd CH_2), 3.42 (m, 2H, β-CH_2), 3.93, 4.03 (2m, 2H, nbd aliph. CH), 4.12 (t, 1H, α-CH), 4.47, 4.70, 4.78, 5.07 (4t, 4H, nbd olef. CH), 7.05, 7.55 (2s, 2H, Im-CH) ppm.

[RuCl(L-his)(cod)] (2)

Preparation with 216 mg (0.77 mmol) $[RuCl_2(cod)]_n$ and 123 mg (0.79 mmol) L-histidine analogous to **1**. *Anal.* Found: C, 41.9; H 4.95; N 10.4. Calc for $C_{14}H_{20}N_3O_2ClRu$ (*M*, 398.9): C, 42.1; H 5.05; N 10.5%. IR: 3240m, 3150s $\nu(NH_2)$, 1640s $\nu(CO)$, 1630s $\delta(NH_2)$. ^1H NMR (D_2O/DSS): 1.38–1.77, 3.21–3.54 (superimposed signals of cod CH_2), 3.77–4.67 (superimposed signals of cod CH, α-CH, β-CH_2), 6.89, 7.10 (2s, 2H, Im–CH).

[RuCl(D,L-his)(PPh_3)$_2$]·1½CH_3OH (3)

264 mg (0.28 mmol) $[RuCl_2(PPh_3)_3]$ and 45 mg (0.29 mmol) D,L-histidine were heated with stirring in 15 ml methanol in the presence of 0.29 mmol NaOMe for 4 h at reflux. The solution was cooled to −30 °C to yield yellow–orange prismatic crystals of **3**. Yield 191 mg (79%). *Anal.* Found: C, 60.4; H 4.90; N 5.0. Calc. for $C_{87}H_{88}N_6O_7P_4Cl_2Ru_2$ (*M*, 1726.6): C, 60.5; H 5.13; N 4.9%. IR: 3350w, 3270w, 3195w $\nu(NH_2)$, 1625s $\nu(CO)$, 1590sh $\delta(NH_2)$. $^{31}P\{^1H\}$ NMR (d_4-methanol, external 85% H_3PO_4 standard): 58.59, 44.70 (2d, 2P). ^1H NMR (d_4-methanol, TMS) 3.03, 3.45 (2m, 2H, β-CH_2), 3.96 (m, 1H, α-CH), 6.72–7.51 (superimposed signals of Ph–H and Im–H).

[$RuCl_2$(L-hisme)(PPh_3)$_2$] (4)

A mixture of 213 mg (0.22 mmol) $[RuCl_2(PPh_3)_3]$ and 113 mg (0.46 mmol) L-histidine methyl ester dihydrochloride was heated with stirring in 15 ml methanol in the presence of 0.95 mmol NaOMe for 3 h at reflux. The solution was reduced in volume to 5 ml and then cooled to −30 °C to yield orange needles of **4**. Yield 130 mg (68%). *Anal.* Found: C, 58.8; H 4.70; N 4.5. Calc. for $C_{43}H_{41}N_3O_2P_2Cl_2Ru$ (*M*, 865.7): C, 59.6; H 4.77; N 4.8%. IR: 3310m, 3150w, $\nu(NH_2)$, 1745s $\nu(CO)$, 1590m $\delta(NH_2)$. $^{31}P\{^1H\}$ NMR (d_4-methanol, external 85% H_3PO_4 standard): 61.08, 43.38 (2d, 2P). ^1H NMR (d_4-methanol, TMS) 3.46, 3.64 (2m, 2H, β-CH_2), 3.59 (s, 3H, CH_3), 4.03 (m, 1H, α-CH), 6.75–7.52 (superimposed signals of Ph-H and Im-H).

[RuCl(D,L-met)(PPh_3)$_2$]·CH_3OH (5)

A mixture of 254 mg (0.27 mmol) $[RuCl_2(PPh_3)_3]$ and 82 mg (0.55 mmol) D,L-methionine were heated with stirring in 20 ml methanol in the presence of 0.30 mmol NaOMe for 25 min at reflux. The solution was reduced in volume to 3 ml and allowed to stand at 7 °C to yield yellow crystals of **5**. Yield 203 mg (85%). *Anal.* Found: C, 59.2; H 5.04; N 1.6. Calc. for $C_{42}H_{44}NO_3P_2SCl_2Ru$ (*M*, 841.4): C, 60.0; H 5.27; N 1.7%. IR: 3330m, 3290w, $\nu(NH_2)$, 1645s $\nu(CO)$, 1625s $\delta(NH_2)$. $^{31}P\{^1H\}$ NMR (d_4-methanol, external 85% H_3PO_4 standard): 42.33, 39.47 (2d, 2P). ^1H NMR (d_4-methanol, TMS) 1.12–1.24 (2m, H, met-CH_2), 2.20 (s, 3H, S–CH_3), 2.42–2.63 (2m, 2H, met-CH_2), 3.62 (m, 1H, met-CH), 7.06–7.50 (m, 30H, Ph–H).

[RuCl(L-metme)$_2$(PPh_3)]Cl·PPh_3 (6)

300 mg (0.31 mmol) $[RuCl_2(PPh_3)_3]$ (**3**) and 126 mg (0.63 mmol) L-methionine methyl ester hydrochloride were heated at reflux in 15 ml methanol in the presence of 0.63 mmol NaOMe for 15 min. The yellow solution was reduced in volume to 4 ml and allowed to stand at −30 °C to yield crystals of **6**. These were recrystallized from CH_2Cl_2/petroleum ether. Yield 160 mg (51%). *Anal.* Found: C, 56.5; H 5.17; N 2.5. Calc. for $C_{48}H_{56}N_2O_4P_2S_2Cl_2Ru$ (*M*, 1022.90): C, 56.4; H 5.52; N 2.7%. IR: 3285m, 3265m, 3220w, 3180w, $\nu(NH_2)$, 1740s $\nu(CO)$, 1585m $\delta(NH_2)$. $^{31}P\{^1H\}$ NMR (d_4-methanol, external 85% H_3PO_4 standard): 46.30 (s, 1P), −7.02 (s, 1P, PPh_3). ^1H NMR (d_4-methanol, TMS) 2.15, 2.35 (2s, 6H, S–CH_3), 2.48–2.60, 2.80–3.02 (mm 8H, β-CH_2, γ-CH_2), 3.57, 3.60 (2s, 6H, $COOCH_3$), 3.61, 3.75 (2m, 2H, α-CH).

[$RuCl_3$(L-metet)(PPh_3)] (**7**)

A mixture of 348 mg (0.36 mmol) [$RuCl_2(PPh_3)_3$] and 162 mg (0.70 mmol) L-methionine methyl ester hydrochloride was refluxed for 18 h in 20 ml methanol under air. After filtration the solution was reduced in volume to 5 ml to yield red crystals of **7** at r.t. Yield 110 mg (47.2%). *Anal.* Found: C, 46.5; H 4.59; N 2.1. Calc. for $C_{25}H_{30}NO_2PCl_3Ru$ (*M*, 647.0): C, 46.4; H 4.67; N 2.2%. IR: 3320m, 3260w, $\nu(NH_2)$, 1770s, 1725m ν(CO), 1600w $\delta(NH_2)$.

X-ray structural analyses of 1, 3, 6 and 7

Crystal and refinement data are summarized in Table 1. The asymetric unit of **1** contains one methanol solvate molecule, that of **3** 1.5 methanol molecules. In the crystal lattice of **5** the complex [RuCl(L-metme)$_2$(PPh_3)] and PPh_3 are present in a 1:1 ratio. Unit cell constants were obtained for the crystals from least-squares fits to the settings of 25 reflections centred on an Enraf-Nonius CAD4 diffractometer. Intensities were collected on the diffractometer at varied scan rates in either the ω– or θ–2θ mode with graphite-monochromated radiation. Mo Kα radiation was employed for the crystals of **1** and **7** with respective dimensions of $0.32\times0.25\times0.06$ and $0.55\times0.23\times0.13$ mm. For the smaller crystals of **3** and **6** ($0.32\times0.25\times0.06$ and $0.30\times0.16\times0.04$ mm, respectively) Cu Kα radiation was used for the data collection. Empirical absorption corrections were applied to the reflection intensities. The structures were solved by Patterson syntheses and refined by full-matrix least-squares. The positions of the methanol solvate molecules in **1** and **3** were revealed by difference syntheses. Carbon atom C200 in **3** lies on a crystallographic symmetry plane with the result that 0200 of this methanol molecule is disordered with a site occupation factor of 0.5. Hydrogen atoms were included at geometrically calculated positions with group isotropic temperature factors. Anisotropic temperature factors were introduced for all non-hydrogen atoms (with the exception of the methanol C and O atoms) for **1** and **3**. Use of such components was restricted to the heavier atoms (Ru, Cl, S, P) in **6**. With the exception of the phenyl carbon atoms all non-hydrogen atoms were refined anisotropically in **7**. Terminal reliability indices are listed in Table 1, where $R_w=[\Sigma w(F_o-F_c)^2/\Sigma wF_o^2]^{1/2}$; weights were applied using the expression $w=(\sigma^2(F_o)+p^2F_o^2)^{-1}$, with values of p as given in Table 1. Calculations were performed with SHELX-76 [12] with the SDP suite (Enraf-Nonius) and with local programs. Diagrams were drawn with RSPLOT [13]. Atom positional parameters with equivalent isotropic temperature factors are listed in Table 2; bond distances and angles to the ruthenium atoms in Table 3.

Discussion

The molecular structure of [RuCl(L-his)(nbd)] (**1**), in which the histidinate anion is present as a facial tridentate ligand, is depicted in Fig. 1. N2 of the amino function is positioned *trans* to the chlorine atom Cl1, so that the coordination may be described as *OC*-6-45 [14]. Alternative ligand arrangements would be *OC*-6-35 (N5 *trans* to Cl1) or *OC*-6-25 (O1 *trans* to Cl1). N2 is displaced −0.61 Å from the best least-squares plane through the remaining atoms of the five-membered

TABLE 1. Crystal and refinement data

Compound	**1**	**3**	**6**	**7**
Space group	$P2_1$	$P2_1/c$	$P2_1$	$P2_1$
a (Å)	9.980(1)	17.705(2)	14.800(2)	20.720(4)
b (Å)	11.381(1)	11.583(2)	10.322(4)	8.684(2)
c (Å)	7.002(1)	21.056(3)	17.190(3)	15.225(3)
α (°)	90	90	90	90
β (°)	101.32(1)	112.88(1)	115.31(1)	93.40(2)
γ (°)	90	90	90	90
V (Å^3)	779.9(3)	3979(2)	2374(2)	2735(2)
Z	2	4	2	4
D_c (g cm^{-3})	1.77	1.44	1.43	1.57
Radiation	Mo Kα	Cu Kα	Cu Kα	Mo Kα
μ(cm^{-1})	11.7	50.1	56.1	10.1
Scan type	θ–2θ	ω	θ–2θ	ω
$2\theta_{max}$ (°)	50	110	120	50
Reflections collected	1558	5167	3755	5146
Reflections observed	1331	3666	2196	4536
Rejection criterion	$F_o^2<2\sigma(F_o^2)$	$F_o^2<2\sigma(F_o^2)$	$F_o^2<2\sigma(F_o^2)$	$F_o^2<2\sigma(F_o^2)$
R	0.045	0.053	0.083	0.035
R_w	0.045	0.051	0.078	0.035
p	0.014	0.014	0.032	0.014

TABLE 2. Atom positional parameters with equivalent isotropic temperature factors ($Å^2 \times 10^3$)

Atom	x/a	y/b	z/c	U
Compound **1**				
Ru1	0.7577(1)	0.0000	0.1479(1)	28(1)
Cl1	0.7253(3)	−0.0617(3)	0.4671(4)	45(2)
O1	0.8688(7)	−0.1586(7)	0.1545(11)	35(4)
O2	1.0722(8)	−0.2208(7)	0.1085(13)	47(5)
N2	0.8584(8)	0.0225(9)	−0.0887(12)	31(5)
N5	0.9370(9)	0.0853(9)	0.2962(12)	34(5)
N7	1.0679(10)	0.1993(10)	0.5072(16)	50(6)
C1	0.9756(12)	−0.1509(10)	0.0781(16)	36(6)
C2	0.9886(13)	−0.0387(10)	−0.0443(16)	39(6)
C3	1.1023(11)	0.0383(10)	0.0666(17)	38(6)
C4	1.0635(11)	0.0956(12)	0.2432(17)	40(6)
C6	0.9445(12)	0.1494(12)	0.4535(17)	43(6)
C8	1.1470(14)	0.1671(13)	0.3779(20)	55(7)
C11	0.6090(13)	0.1296(10)	0.1929(20)	42(6)
C12	0.6499(12)	0.1529(11)	0.0227(18)	39(6)
C13	0.5498(11)	0.0901(12)	−0.1428(20)	42(7)
C14	0.5892(12)	−0.0382(10)	−0.0921(17)	36(6)
C15	0.5448(12)	−0.0637(11)	0.0798(17)	36(6)
C16	0.4803(12)	0.0502(12)	0.1359(18)	41(6)
C17	0.4143(12)	0.0973(14)	−0.0608(20)	54(8)
O100	0.3252(26)	0.8116(25)	0.4065(36)	215(10)
C100	0.2903(34)	0.8957(38)	0.5398(51)	185(13)
Compound **3**				
Ru1	0.2790(1)	0.1590(1)	0.1722(1)	29(1)
Cl1	0.2143(1)	−0.0302(2)	0.1547(1)	52(1)
P1	0.3147(1)	0.1527(2)	0.2913(1)	33(1)
P2	0.1597(1)	0.2611(2)	0.1367(1)	32(1)
O1	0.3907(3)	0.0691(5)	0.1905(3)	42(3)
O2	0.4928(3)	0.0702(6)	0.1537(3)	60(4)
N2	0.2772(3)	0.1327(5)	0.0705(3)	38(3)
N5	0.3466(3)	0.3101(5)	0.1770(3)	31(3)
N7	0.4227(4)	0.4615(6)	0.2199(4)	44(4)
C1	0.4204(5)	0.0888(7)	0.1449(4)	42(5)
C2	0.3634(4)	0.1419(7)	0.0762(4)	43(5)
C3	0.3865(5)	0.2681(7)	0.0741(4)	45(5)
C4	0.3917(4)	0.3342(7)	0.1370(4)	37(4)
C6	0.3668(4)	0.3888(7)	0.2245(4)	33(4)
C8	0.4388(5)	0.4266(8)	0.1643(5)	51(5)
C112	0.2631(3)	−0.0100(6)	0.3696(3)	63(6)
C113	0.2631(3)	−0.1206(6)	0.3958(3)	87(7)
C114	0.3027(3)	−0.2107(6)	0.3774(4)	98(8)
C115	0.3424(3)	−0.1902(6)	0.3327(3)	80(7)
C116	0.3423(3)	−0.0796(6)	0.3065(3)	59(5)
C111	0.3027(3)	0.0105(6)	0.3249(3)	41(4)
C122	0.4508(3)	0.1464(5)	0.4154(2)	50(5)
C123	0.5319(3)	0.1665(5)	0.4598(2)	65(5)
C124	0.5877(3)	0.2102(5)	0.4340(2)	64(6)
C125	0.5624(3)	0.2338(5)	0.3638(2)	51(5)
C126	0.4813(3)	0.2137(5)	0.3194(2)	38(4)
C121	0.4255(3)	0.1700(5)	0.3452(2)	35(4)
C132	0.1911(3)	0.2394(5)	0.3304(3)	62(6)
C133	0.1552(3)	0.3207(5)	0.3589(3)	88(8)
C134	0.1997(3)	0.4177(5)	0.3924(3)	94(8)
C135	0.2799(3)	0.4333(5)	0.3975(3)	73(6)
C136	0.3158(3)	0.3519(5)	0.3690(3)	52(5)
C131	0.2714(3)	0.2549(5)	0.3355(3)	43(5)
C212	0.2054(3)	0.4725(4)	0.1011(2)	41(4)
C213	0.2334(3)	0.5861(4)	0.1135(2)	52(5)
C214	0.2352(3)	0.6437(4)	0.1723(2)	56(5)
C215	0.2091(3)	0.5876(4)	0.2187(2)	53(5)
C216	0.1811(3)	0.4739(4)	0.2064(2)	40(4)
C211	0.1792(3)	0.4164(4)	0.1476(2)	30(4)
C222	0.0480(3)	0.3406(4)	0.0044(3)	45(4)
C223	−0.0094(3)	0.3222(4)	−0.0624(3)	52(5)
C224	−0.0221(3)	0.2112(4)	−0.0903(3)	52(5)
C225	0.0226(3)	0.1186(4)	−0.0514(3)	47(5)
C226	0.0800(3)	0.1369(3)	0.0154(4)	42(5)
C221	0.0927(3)	0.2479(4)	0.0433(3)	34(4)
C232	0.0228(3)	0.3217(4)	0.1682(3)	56(5)
C233	−0.0405(3)	0.2968(4)	0.1899(3)	79(7)
C234	−0.0494(3)	0.1852(4)	0.2109(3)	98(9)
C235	0.0049(3)	0.0985(4)	0.2102(3)	88(8)
C236	0.0682(3)	0.1234(4)	0.1884(3)	56(5)
C231	0.0771(3)	0.2350(4)	0.1674(3)	40(4)
O100	0.2254(4)	−0.3601(6)	0.5238(4)	96(2)
C100	0.1467(6)	−0.3193(10)	0.4811(5)	78(3)
O200	0.4486(13)	0.5691(21)	0.4491(12)	175(9)
C200	0.5000	0.5000	0.5000	164(9)
Compound **6**				
Ru1	−0.1812(1)	0.0000	−0.2269(1)	22(1)
Cl1	−0.3542(5)	−0.0692(7)	−0.2754(4)	36(3)
Cl2	−0.0401(5)	0.3635(8)	−0.1093(4)	49(4)
S11	−0.1242(5)	−0.2149(8)	−0.2089(4)	34(4)
S21	−0.1725(4)	0.0402(6)	−0.0834(4)	29(4)
P1	−0.1920((4)	−0.0072(11)	−0.3655(4)	28(3)
P2	0.2595(5)	−0.4058(9)	−0.1467(5)	50(5)
O11	0.1666(15)	0.1260(23)	−0.1348(13)	72(6)
O12	0.2194(13)	0.0542(19)	−0.0018(12)	58(6)
O21	−0.3178(14)	0.4288(21)	−0.3262(12)	57(6)
O22	−0.4385(15)	0.4070(24)	−0.2837(13)	71(6)
N11	−0.0277(13)	0.0660(21)	−0.1708(12)	31(5)
N21	−0.2266(13)	0.2013(20)	−0.2491(12)	25(5)
C11	0.1519(17)	0.0741(29)	−0.0814(15)	50(8)
C12	0.0531(15)	0.0027(28)	−0.0971(13)	42(6)
C13	0.3210(21)	0.1056(38)	0.0200(21)	79(11)
C14	0.0686(18)	−0.1406(24)	−0.1102(17)	38(7)
C15	−0.0093(15)	−0.2288(29)	−0.1096(14)	48(8)
C16	−0.2005(21)	−0.3303(29)	−0.1852(19)	61(9)
C21	−0.3550(19)	0.3726(27)	−0.2880(17)	47(8)
C22	−0.3142(15)	0.2450(23)	−0.2363(14)	26(6)
C23	−0.4886(23)	0.5195(36)	−0.3401(21)	87(11)
C24	−0.2891(19)	0.2606(25)	−0.1404(15)	40(7)
C25	−0.2835(15)	0.1346(23)	−0.0988(15)	31(6)
C26	−0.2051(20)	−0.1016(24)	−0.0399(16)	42(7)
C122	−0.3656(11)	0.1446(17)	−0.4408(10)	31(6)
C123	−0.4303(11)	0.2340(17)	−0.4987(10)	53(8)
C124	−0.4016(11)	0.3001(17)	−0.5552(10)	56(8)
C125	−0.3080(11)	0.2768(17)	−0.5538(10)	65(10)
C126	−0.2433(11)	0.1874(17)	−0.4959(10)	48(8)
C121	−0.2720(11)	0.1213(17)	−0.4394(10)	27(6)
C132	−0.0176(13)	−0.0889(16)	−0.3738(11)	46(8)
C133	0.0783(13)	−0.0735(16)	−0.3690(11)	66(10)
C134	0.1214(13)	0.0494(16)	−0.3567(11)	62(9)
C135	0.0687(13)	0.1569(16)	−0.3490(11)	65(9)
C136	−0.0272(13)	0.1416(16)	−0.3537(11)	36(7)
C131	−0.0703(13)	0.0187(16)	−0.3661(11)	26(5)

(*continued*)

(*continued*)

TABLE 2 (*continued*)

Atom	*x/a*	*y/b*	*z/c*	*U*
C212	0.4160(12)	−0.3070(15)	−0.1886(11)	42(8)
C213	0.4673(12)	−0.2055(15)	−0.2055(11)	40(7)
C214	0.4323(12)	−0.0787(15)	−0.2112(11)	67(10)
C215	0.3460(12)	−0.0535(15)	−0.2000(11)	77(11)
C216	0.2947(12)	−0.1549(15)	−0.1831(11)	61(9)
C211	0.3297(12)	−0.2817(15)	−0.1775(11)	35(6)
C222	0.4105(15)	−0.5703(19)	−0.0510(10)	73(10)
C223	0.4789(19)	−0.6715(19)	−0.0336(10)	71(10)
C224	0.4770(15)	−0.7500(19)	0.1003(10)	63(9)
C225	0.4068(15)	−0.7272(19)	−0.1846(10)	59(9)
C226	0.3383(15)	−0.6260(19)	−0.2020(10)	74(11)
C221	0.3402(15)	−0.5476(19)	−0.1353(10)	36(7)
C232	0.0669(12)	−0.4807(21)	−0.2377(8)	45(6)
C233	−0.0237(12)	−0.4972(21)	−0.3099(8)	64(8)
C234	−0.0293(12)	−0.4756(21)	−0.3920(8)	52(7)
C235	0.0557(12)	−0.4375(21)	−0.4018(8)	52(8)
C236	0.1463(12)	−0.4209(21)	−0.3295(8)	39(7)
C231	0.1519(12)	−0.4426(21)	−0.2475(8)	53(8)
C112	−0.2818(12)	−0.2502(17)	−0.4140(8)	33(6)
C113	−0.3196(12)	−0.3539(17)	−0.4710(8)	52(8)
C114	−0.3172(12)	−0.3501(17)	−0.5512(8)	52(8)
C115	−0.2771(12)	−0.2427(17)	−0.5745(8)	61(9)
C116	−0.2393(12)	−0.1390(17)	−0.5176(8)	41(7)
C111	−0.2416(12)	−0.1428(17)	−0.4374(8)	25(6)
Compound **7**				
Ru1	0.1341(1)	0.0000	0.2838(1)	30(1)
Ru2	0.3736(1)	0.0305(1)	−0.2113(1)	33(1)
Cl11	0.0255(1)	0.0040(3)	0.2335(1)	47(1)
Cl12	0.2381(1)	−0.0369(3)	0.3439(1)	52(1)
Cl13	0.1314(1)	0.2537(2)	0.3378(1)	44(1)
Cl21	0.2720(1)	0.0118(3)	−0.1532(1)	47(1)
Cl22	0.4770(1)	0.0111(3)	−0.2613(1)	53(1)
Cl23	0.3886(1)	0.2896(2)	−0.1720(1)	48(1)
S11	0.1285(1)	−0.2597(3)	0.2329(1)	52(1)
S21	0.3585(1)	−0.2403(3)	−0.2298(1)	54(1)
P11	0.1707(1)	0.0801(2)	0.1486(1)	32(1)
P21	0.3268(1)	0.0893(2)	−0.3508(1)	36(1)
O11	0.0065(3)	−0.3132(10)	0.5460(4)	92(5)
O12	0.0744(3)	−0.1247(7)	0.5814(3)	51(3)
O21	0.4711(3)	0.0103(12)	0.0826(4)	98(5)
O22	0.4042(3)	−0.1605(8)	0.1324(3)	59(4)
N11	0.1028(3)	−0.0651(7)	0.4144(4)	38(3)
N21	0.4209(3)	−0.0062(9)	−0.0828(3)	46(3)
C11	0.0558(4)	−0.1892(9)	0.4291(4)	42(4)
C12	0.0420(4)	−0.2160(10)	0.5243(5)	46(4)
C13	0.0620(5)	−0.1530(13)	0.6741(5)	69(6)
C14	0.0965(5)	−0.0406(19)	0.7282(6)	117(10)
C15	0.0763(4)	−0.3436(10)	0.3928(5)	52(5)
C16	0.0687(4)	−0.3546(10)	0.2930(5)	57(5)
C17	0.1990(4)	−0.3706(10)	0.2717(7)	80(7)
C21	0.3955(4)	−0.1128(9)	−0.0187(5)	43(4)
C22	0.4297(4)	−0.0818(12)	0.0696(5)	55(5)
C23	0.4284(5)	−0.1263(14)	0.2224(5)	80(7)
C24	0.3923(5)	−0.2095(21)	0.2813(6)	121(10)
C25	0.4008(4)	−0.2799(10)	−0.0487(5)	59(5)
C26	0.3508(5)	−0.3204(11)	−0.1226(5)	69(6)
C27	0.4299(5)	−0.3353(11)	−0.2604(6)	78(7)
C111	0.1172(3)	0.2056(9)	0.0808(4)	38(2)
C112	0.1214(4)	0.2114(10)	−0.0101(5)	50(2)
C113	0.0813(4)	0.3112(11)	−0.0591(6)	57(2)

(*continued*)

TABLE 2 (*continued*)

Atom	*x/a*	*y/b*	*z/c*	*U*
C114	0.0395(4)	0.4082(11)	−0.0203(5)	58(2)
C115	0.0368(4)	0.4059(10)	0.0695(5)	55(2)
C116	0.0749(4)	0.3014(10)	0.1196(5)	45(2)
C121	0.2466(3)	0.1864(8)	0.1478(4)	35(2)
C122	0.2714(3)	0.2672(9)	0.2209(5)	45(2)
C123	0.3262(4)	0.3591(10)	0.2162(6)	56(2)
C124	0.3571(4)	0.3661(10)	0.1390(5)	56(2)
C125	0.3334(4)	0.2866(11)	0.0652(5)	55(2)
C126	0.2783(3)	0.1989(9)	0.0704(5)	43(2)
C131	0.1854(3)	−0.0831(9)	0.0796(4)	38(2)
C132	0.2424(4)	−0.1673(10)	0.0950(5)	49(2)
C133	0.2494(4)	−0.3093(12)	0.0543(6)	67(3)
C134	0.2013(4)	−0.3645(13)	−0.0023(6)	73(3)
C135	0.1456(4)	−0.2836(12)	−0.0197(6)	65(3)
C136	0.1367(4)	−0.1459(10)	0.0228(5)	56(2)
C211	0.3778(4)	0.1921(9)	−0.4261(5)	41(2)
C212	0.4245(4)	0.2934(10)	−0.3945(5)	50(2)
C213	0.4618(4)	0.3758(11)	−0.4500(6)	61(2)
C214	0.4521(4)	0.3521(11)	−0.5402(6)	58(2)
C215	0.4065(4)	0.2528(12)	−0.5712(6)	67(3)
C216	0.3669(4)	0.1715(11)	−0.5162(5)	56(2)
C221	0.2527(3)	0.2051(9)	−0.3550(5)	38(2)
C222	0.2108(4)	0.2073(10)	−0.4287(5)	48(2)
C223	0.1546(4)	0.2951(11)	−0.4301(5)	53(2)
C224	0.1402(4)	0.3784(10)	−0.3599(5)	56(2)
C225	0.1823(4)	0.3838(11)	−0.2867(6)	61(2)
C226	0.2382(4)	0.2969(10)	−0.2849(5)	48(2)
C231	0.3049(4)	−0.0857(9)	−0.4090(5)	43(2)
C232	0.2442(4)	−0.1533(11)	−0.4018(6)	56(2)
C233	0.2304(5)	−0.2994(13)	−0.4370(6)	77(3)
C234	0.2760(5)	−0.3757(13)	−0.4770(7)	79(3)
C235	0.3351(5)	−0.3151(13)	−0.4869(7)	80(3)
C236	0.3524(4)	−0.1670(11)	−0.4515(6)	57(2)

histidinate metallocyclus. The envelope conformation is characterized by the distances of these four atoms from the plane: Ru1 0.02, 0.1 −0.06, C1 0.07, C2 −0.03 Å. A half-chair conformation is observed for the adjacent six-membered metallocyclus with N2 displaced −0.92 Å from the best plane through the remaining five atoms. Distances from this plane are: Ru1 −0.04, N5 0.05, C4 −0.01, C3 −0.05, C2 0.05 Å.

Complex **2** [RuCl(L-his)(cod)] with identical stoichiometry to **1** may be prepared by the analogous reaction of $[RuCl(cod)]_n$ with L-histidine in aqueous solutions at reflux. The positions of the $\nu(NH_2)$ and $\nu(CO)$ bands in the IR spectrum of **2** are typical for coordinated amino and carboxylate functions. Although the imidazole proton resonances in the ^1H NMR spectrum (D_2O/DSS) of **2** do not allow the unequivocal establishment of N(imidazole) participation in the coordination sphere of the ruthenium atom, this may reasonably be assumed, in light of the crystal structure of **1**. We have recently observed that the reaction of $[RuCl_2(diene)]_n$ (diene = nbd, cod) with L-histidine methyl ester in neutral aqueous solution at reflux also

TABLE 3. Bond distances (Å) and angles (°) to the ruthenium atoms

1			
Ru1–C11	2.425(3)	Ru1–O1	2.114(8)
Ru1–N2	2.114(8)	Ru1–N5	2.120(8)
Ru1–C11	2.159(11)	Ru1–C12	2.141(12)
Ru1–C14	2.175(11)	Ru1–C15	2.206(11)
Cl1–Ru1–O1	84.1(2)	Cl1–Ru1–N2	158.0(2)
Cl1–Ru1–N5	86.2(2)	Cl1–Ru1–C11	81.0(4)
Cl1–Ru1–C12	117.7(3)	Cl1–Ru1–C14	115.6(3)
Cl1–Ru1–C15	78.9(3)	N2–Ru1–O1	78.1(3)
N5–Ru1–O1	89.5(3)	N5–Ru1–N2	81.0(3)
C11–Ru1–O1	162.3(4)	C11–Ru1–N2	118.5(4)
C11–Ru1–N5	98.8(4)	C12–Ru1–O1	157.3(4)
C12–Ru1–N2	81.9(4)	C12–Ru1–N5	97.8(4)
C14–Ru1–O1	99.7(4)	C14–Ru1–N2	80.4(4)
C14–Ru1–N5	157.0(4)	C14–Ru1–C11	78.5(5)
C14–Ru1–C12	66.2(5)	C15–Ru1–O1	101.7(4)
C15–Ru1–N2	117.1(4)	C15–Ru1–N5	160.2(4)
C15–Ru1–C11	66.2(5)	C15–Ru1–C12	78.1(5)
C1–O1–Ru1	114.0(7)	C2–N2–Ru1	108.4(6)
C4–N5–Ru1	129.2(7)	C6–N5–Ru1	124.7(8)
3			
Ru1–Cl1	2.433(2)	Ru1–P1	2.338(2)
Ru1–P2	2.277(2)	Ru1–O1	2.134(5)
Ru1–N2	2.150(6)	Ru1–N5	2.101(6)
P1–Ru1–Cl1	92.8(1)	P2–Ru1–Cl1	95.5(1)
P2–Ru1–P1	101.4(1)	O1–Ru1–Cl1	86.3(2)
O1–Ru1–P1	86.9(1)	O1–Ru1–P2	171.4(1)
N2–Ru1–Cl1	84.1(2)	N2–Ru1–P1	163.1(2)
N2–Ru1–P2	95.4(2)	N2–Ru1–O1	76.4(2)
N5–Ru1–Cl1	169.5(2)	N5–Ru1–P1	93.6(2)
N5–Ru1–P2	91.3(2)	N5–Ru1–O1	85.8(2)
N5–Ru1–N2	87.3(2)		
6			
Ru1–Cl1	2.436(6)	Ru1–P1	2.321(6)
Ru1–S11	2.346(8)	Ru1–S21	2.450(6)
Ru1–N11	2.16(2)	Ru1–N21	2.17(2)
S11–Ru1–Cl1	91.9(2)	S21–Ru1–Cl1	89.4(2)
S21–Ru1–S11	99.6(2)	P1–Ru1–Cl1	92.2(2)
P1–Ru1–S11	88.2(3)	P1–Ru1–S21	172.0(3)
N11–Ru1–Cl1	174.0(5)	N11–Ru1–S11	89.4(6)
N11–Ru1–S21	84.5(5)	N1–Ru1–P1	93.8(5)
N21–Ru1–Cl1	91.1(5)	N21–Ru1–S11	175.4(5)
N21–Ru1–S21	83.9(5)	N21–Ru1–P1	88.2(5)
N21–Ru1–N11	87.9(8)		
7			
Ru1–Cl11	2.334(2)	Ru2–Cl21	2.336(2)
Ru1–Cl12	2.313(2)	Ru2–Cl22	2.323(2)
Ru1–Cl13	2.353(2)	Ru2–Cl23	2.344(2)
Ru1–S11	2.385(2)	Ru2–S21	2.387(3)
Ru1–P11	2.341(2)	Ru2–P21	2.339(2)
Ru1–N11	2.202(6)	Ru2–N21	2.160(6)
Cl12–Ru1–Cl11	171.6(1)	Cl22–Ru2–Cl21	171.3(1)
Cl13–Ru1–Cl11	93.3(1)	Cl23–Ru2–Cl21	94.6(1)
Cl13–Ru1–Cl12	91.8(1)	Cl23–Ru2–Cl22	92.4(1)
S11–Ru1–Cl11	83.1(1)	S21–Ru2–Cl21	82.0(1)
S11–Ru1–Cl12	91.3(1)	S21–Ru2–Cl22	90.4(1)
S11–Ru1–Cl13	175.5(1)	S21–Ru2–Cl23	172.0(1)
P11–Ru1–Cl11	93.6(1)	P21–Ru2–Cl21	91.4(1)
P11–Ru1–Cl12	92.7(1)	P21–Ru2–Cl22	93.4(1)
P11–Ru1–Cl13	92.6(1)	P21–Ru2–Cl23	93.7(1)
P11–Ru1–S11	90.4(1)	P21–Ru2–S21	93.7(1)
N11–Ru1–Cl11	88.3(2)	N21–Ru2–Cl21	91.0(2)
N11–Ru1–Cl12	85.7(2)	N21–Ru2–Cl22	84.7(2)
N11–Ru1–Cl13	84.9(2)	N21–Ru2–Cl23	82.2(2)
N11–Ru1–S11	92.2(2)	N21–Ru2–S21	90.6(2)
N11–Ru1–P11	176.9(2)	N21–Ru2–P21	175.4(2)

(*continued*)

TABLE 3 (*continued*)

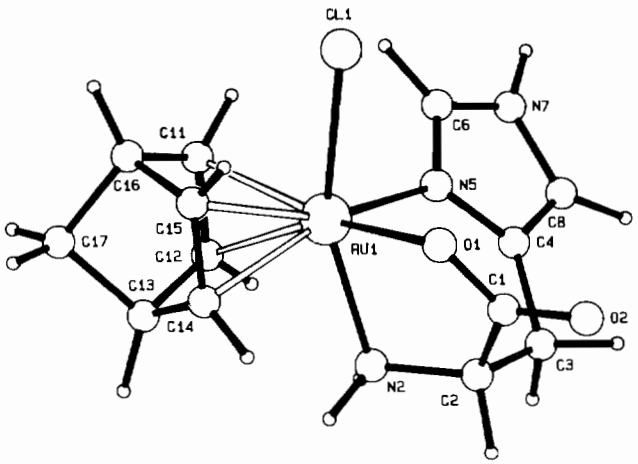

Fig. 1. Molecular structure of [RuCl(L-his)(η^4-nbd)] (**1**).

yields the complexes [RuCl(L-his)(diene)] **1** and **2**, as a result of the hydrolysis of the ester function [15].

Reaction of $[RuCl_2(PPh_3)_3]$ with D,L-histidine in methanol at reflux leads to the formation of the complex $[RuCl(D,L\text{-his})(PPh_3)_2]$ (**3**), which also contains a facially coordinated tridentate histidinate ligand, as established by an X-ray structural analysis (Fig. 2). In contrast to **1**, N5 of the imidazole ring is now sited *trans* to Cl1. Alternative ligand arrangements to this *OC*-6-45 coordination would be *OC*-6-54 (N2 *trans* to Cl1) and *OC*-6-35 (01 *trans* to Cl1). **3** crystallizes as a racemate, so that molecules with Ru_R,C_S (Fig. 2) and Ru_S,C_R configurations are present in the unit cell. The observed *OC*-6-45 coordination geometry would not be possible for an Ru_R,C_R (or Ru_S,C_S) configuration. In contrast to complex **1** the six-membered metallocyclus adopts a distorted conformation in **3** with C2 and N2 displaced 0.45 and −0.50 Å from the best least-squares plane through the remaining four atoms. Distances from this plane are: Ru1 0.02, N5 −0.05, C4 0.06, C3 −0.03 Å. A distorted half-chair conformation is observed for the five-membered metallocyclus.

Comparison of the Ru–P distances in **3** shows that the bond trans to the amino nitrogen N2 (2.338(2) Å) is significantly longer than that *trans* to the carboxylate oxygen O1 (2.277(2) Å). An AB quartet is observed

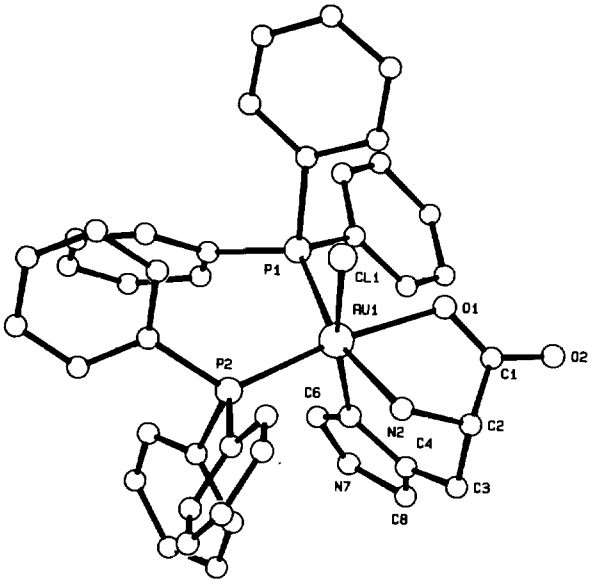

Fig. 2. Molecular structure of [RuCl(D,L-his)$(PPh_3)_2$] (**3**).

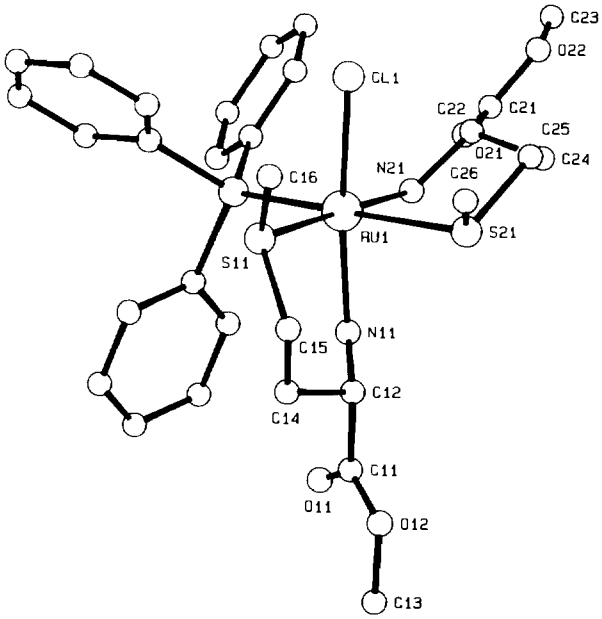

Fig. 3. Molecular structure of [RuCl(L-metme)$_2$$(PPh_3)$]Cl (**6**).

for **3** in the $^{31}P\{^1H\}$ NMR spectrum taken in d_4-methanol. A tentative assignment of signal at higher field (δ 44.70 ppm) to P2 *trans* to 01 may be made, as an increased degree of d_π–p_π backbonding will be predicted for the shorter Ru1–P2 bond. The resonance at lower field (δ 58.59 ppm) is then assigned to P1 *trans* to N2.

L-Histidine methyl ester is present as a bidentate ligand in [$RuCl_2$(L-hisme)$(PPh_3)_2$] (**4**). Phosphorus resonances at 61.08 and 43.38 ppm are observed in the $^{31}P\{^1H\}$ NMR spectrum (d_4-methanol) of this complex (AB system). If, in analogy to **3** and [Ru(L-ala)$_2$$(PPh_3)_2$] ($\delta$ 55.22 ppm) the signal at lower field (61.08 ppm) is assigned to a phosphorus atom *trans* to an amino nitrogen, two possible coordination geometries *OC*-6-14 (Cl atoms *trans* to one another) and *OC*-6-23 (Cl atom *cis* to one another) remain. We prefer the latter geometry as this would allow the assignment of the higher field resonance at 43.38 ppm to a phosphorus atom *trans* to chlorine.

Methionine is also capable of coordinating as a facial tridentate ligand as in [RuCl(D,L-met)(nbd)] [4]. Reaction of [$RuCl_2(PPh_3)_3$] with D,L-methionine or L-methionine methyl ester in methanol leads to the formation of [RuCl(D,L-met)$(PPh_3)_2$]·CH_3OH (**5**) and [RuCl(L-metme)$_2$$(PPh_3)$]Cl·$PPh_3$ (**6**), respectively. The molecular structure of **6** is depicted in Fig. 3; a non-coordinated PPh_3 molecule is also present in the asymmetric unit. The thioether sulfur atoms S11 and S21 adopt coordination sites *trans* to N21 and P1, respectively, so that the octahedral geometry may be described as *OC*-6-44. A *A*-configuration with individual atom chiralities Ru_R, $S11_R$, $S21_R$, $C11_S$, $C21_S$ was established for **6** by the X-ray structural analysis. Distorted chair conformations are adopted by both six-membered rings in **6**. Atoms Ru1 and C14 are displaced 0.89 and −0.72 Å, respectively, from the best least-squares plane through S11 (−0.02), C15 (0.02), N11 (0.02) and C12 (−0.02). Distances (Å) from the plane are provided in parentheses for these latter atoms. In the second ring Ru1 and C24 adopt positions −1.18 and 0.76 Å, respectively, from the best plane through the remaining atoms. Displacements from this plane are −0.02 (S21), 0.03 (C25), 0.03 (N21) and −0.03 (C22) Å, respectively.

A marked *trans*-influence is apparent for the Ru–S distances in **6**. The bond length Ru1–S11 (2.346(8)) is markedly shorter than Ru1–S21 (2.450(6) Å). The former bond is sited *trans* to the amino nitrogen atom N21 the latter bond *trans* to the triphenylphosphine ligand. A pronounced d_π–p_π backbonding component will te expected for the bond Ru1–P1 leading to a reduction of the analogous orbital interaction and thereby to a relative lengthening of the Ru1–S21 bond in *trans* position. Phosphorus resonances at 46.30 and −7.02 ppm are observed for P1 and the uncoordinated phosphorus atom P2 in the $^{31}P\{^1H\}$ NMR spectrum of **6** (d_4-methanol).

Crystals of [RuCl(D,L-met)$(PPh_3)_2$]·CH_3OH (**5**) suitable for an X-ray structural analysis could not be grown. However, it is reasonable to assume that the D,L-methionate anion is present as a facial tridentate ligand displaying the N,O,S-coordination mode. Three octahedral geometries are possible for **5**, namely *OC*-6-25 (S *trans* to Cl), *OC*-6-53 (N *trans* to Cl) and *OC*-6-43 (O*trans* to Cl). A tentative assignment of the *OC*-6-53 coordination geometry is possible by comparison of the phosphorus resonances in the $^{31}P\{^1H\}$ NMR spectrum of **5** (d_4-methanol, 42.33, 39.47 ppm) with those in **3**,

4 and **6**. The low field resonances at 58.59 and 61.08 ppm in **3** and **4**, respectively, were assumed to result from PPh_3 ligands *trans* to amino nitrogen atoms. A signal at 44.70 ppm in **3** was assigned to a phosphorus sited *trans* to a carboxylate oxygen. P1 in **6**, which is positioned *trans* to the thioether sulfur atom S21 displays a resonance at 46.30 ppm. The failure to observe a markedly low field phosphorus resonance ($\delta > 50$ ppm) suggests that the amino nitrogen atom in **5** must be sited *trans* to the chloride ligand, i.e. that an *OC*-6-53 coordination geometry has been adopted.

The presence of π-acceptor ligands such as the dienes cod and nbd or triphenylphosphine leads to a relative stabilization of the oxidation state +2 in ruthenium complexes in aqueous or methanolic solution. In contrast to complexes of the type $[Ru(aa)_2(PPh_3)_2]$ (aaH = glyH, L-alaH, L-valH) [3] or $[RuCl_2(L\text{-hisme})(PPh_3)_2]$ (**4**) and $[RuCl(D,L\text{-met})(PPh_3)_2]\cdot CH_3OH$ (**5**) prepared in this work, $[RuCl(L\text{-metme})_2(PPh_3)]Cl\cdot PPh_3$ (**6**) contains only one coordinated phosphine ligand. During the course of the preparation of **6** we noticed that the colour of the reaction solution changed from yellow to orange–red in the presence of traces of oxygen. Although we were not able to characterize the reaction product under these conditions we were successful in isolating a crystalline product **7** from the analogous reaction between $[RuCl_2(PPh_3)_3]$ and L-methionine ethyl ester carried out in methanol at reflux without an inert atmosphere. **7** is a paramagnetic ruthenium(III) complex, whose molecular structure $[RuCl_3(L\text{-metet})(PPh_3)]$ was established by an X-ray structural analysis. Two independent molecules with *OC*-6-21 geometry are present in the asymmetric unit (Fig. 4). A chair conformation is adopted by the six-membered chelate ring in both molecules. Ru1 and C15 are displaced −0.76 and 0.75 Å from the best plane through the remaining four atoms in the first independent molecule. Similar distances of −0.86 and 0.74 Å are observed for Ru2 and C25 for the analogous least-squares plane in the second molecule. The thioether methyl groups are positioned equatorially to the chelate ring in both independent molecules.

It is well known that coordination through four soft sulfur atoms leads to the formation of ruthenium(II) complexes stable in aqueous or methanolic solutions, e.g. $RuCl_2(DMSO)_4$ [16]. The observation of the facile oxidation of Ru(II) to Ru(III) in bis-chelate triphenylphosphine–ruthenium(II) complexes of methionine esters suggests that the presence of two thioether and one PPh_3 ligand is not sufficient to stabilize the lower oxidation state. In view of this observation it appeared to us to be of interest to study the redox behaviour of **7**. For comparison purposes we have also measured the cyclic voltammogram of $[RuCl(D,L\text{-his})(PPh_3)_2]$ (**4**). In the potential range −0.8 to −1.2 V versus Ag/AgCl, this complex displays a quasi-reversible one-electron transfer wave at 0.53 V versus Ag/Cl ($I_p^A/I_p^c = 1$, $\Delta E_p > 59$ mV). The cyclic voltammogram for **7** taken at a scan speed of 0.20 V s^{-1} in the potential range −0.4 to +0.8 V versus Ag/AgCl is depicted in Fig. 5. In the first scan no electron transfer is observed in the range 0.2–0.8 V. A one-electron transfer process occurs at −0.07 V versus Ag/AgCl and leads, presum-

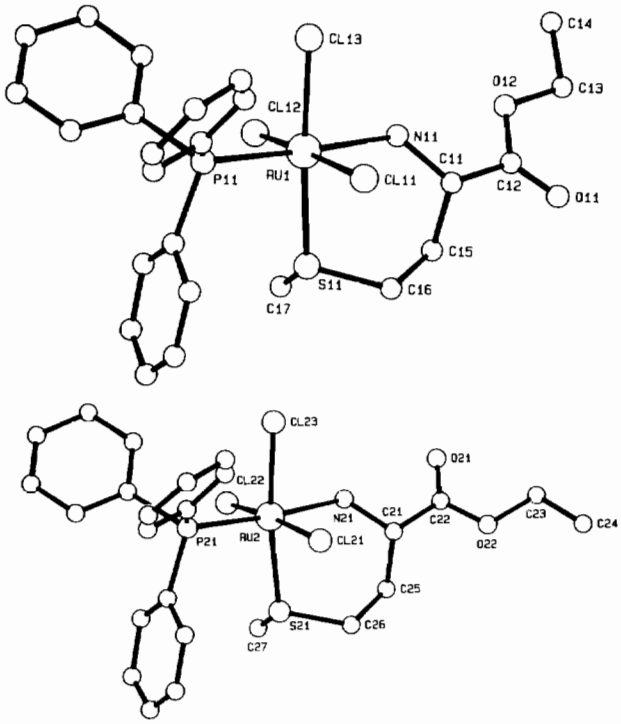

Fig. 4. Molecular structures of the two independent molecules of $[RuCl_3[L\text{-metet}](PPh_3)]$ (**7**).

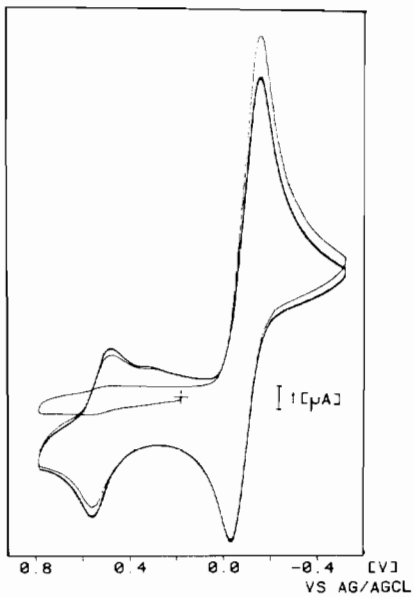

Fig. 5. Cyclic voltammogram of **7** (CH_2Cl_2; 0.1 M $[n\text{-}Bu_4N]PF_6$) at a glassy-carbon electrode (scan speed 0.2 V s^{-1}).

ably, to the formation of $[RuCl_3(L\text{-metet})(PPh_3)]^-$ (**7'**). This anion must be in equilibrium with a second ruthenium(II) species as two one-electron transfer waves are subsequently observed. A tentative explanation would be that dimerization to $[RuCl_2(L\text{-met-et})(PPh_3)]_2$ (**7''**) occurs with loss of a chloride anion, so that the observed cyclic voltammogram for **7** may be described with the help of an ece mechanism. At lower scan rates, the major one-electron-transfer wave for **7/7'** approaches the character of a reversible system (scan speed = 0.01 V s^{-1}, $I_p^A/I_p^c = 0.97$, $\Delta E_p = 65$ mV) and the equilibrium position for **7/7''** lies well to the left.

Acknowledgements

This work was supported by the Fonds der Chemischen Industrie, Frankfurt. We are grateful to Professor Dr K. Wieghardt (Bochum) for the measurement of the cyclic voltammograms and to Degussa AG, Hanau, for a gift of $RuCl_3 \cdot 3H_2O$.

References

1 C. Potvin, L. Davignon and G. Pannetier, *Bull. Soc. Chim. Fr.*, (1974) 507.

2 W. S. Sheldrick and R. Exner, *Inorg. Chim. Acta, 166* (1989) 213.

3 W. S. Sheldrick and R. Exner, *Inorg. Chim. Acta, 175* (1990) 261.

4 W. S. Sheldrick and R. Exner, *J. Organomet. Chem., 386* (1990) 375.

5 W. S. Sheldrick and S. Heeb, *J. Organomet. Chem., 377* (1989) 357.

6 W. S. Sheldrick and R. Exner, *Inorg. Chim. Acta, 184* (1991) 119.

7 H. M. Koepp, H. Wendt and H. Strehlow, *Z. Elektrochem., 64* (1960) 483.

8 M. A. Bennett and G. Wilkinson, *Chem. Ind. (London)*, (1959) 1516.

9 J. Müller and E. O. Fischer, *J. Organomet. Chem., 5* (1966) 275.

10 E. W. Abel, M. A. Bennett and G. Wilkinson, *J. Chem. Soc.*, (1959) 3178.

11 P. S. Hallman, T. A. Stephenson and G. Wilkinson, *Inorg. Synth., 12* (1970) 237.

12 G. M. Sheldrick, *SHELX-76*, computer program for crystal structure determination, University of Cambridge, UK, 1976.

13 W. S. Sheldrick, *RSPLOT*, a computer program for molecule and lattice plots, TU Braunschweig, FRG, 1975.

14 T. E. Sloan, *Top Stereochem., 12* (1981) 1.

15 W. S. Sheldrick and R. Exner, unpublished results.

16 I. P. Evans, A. Spencer and G. Wilkinson, *J. Chem. Soc., Dalton Trans.*, (1973) 204.